Real-space renormalization-group analysis for finite ferromagnetic systems

L. G. Dunfield and J. Noolandi
Xerox Research Center of Canada, 2480 Dunwin Drive, Mississauga, Ontario, Canada, L5L 1J9
(Received 27 December 1979)

The real-space renormalization-group transformation based on the cumulant expansion is modified for systems with free-surface boundary conditions. A discussion is given of the accuracy and limitations of the method and of the extension to higher orders in the cumulant expansion. Free energies and heat capacities of ferromagnetic strips ($n \times \infty$) and slabs ($n \times \infty \times \infty$) are determined over a wide temperature range. Exact results are obtained by a transfer matrix technique for strips with $n \leq 8$, and compared to the renormalization results. The critical or pseudocritical behavior is found to approach the bulk limit as $n \to \infty$ according to a simple power law $|T_c(n) - T_c(\infty)| \propto n^{-\lambda}$, where the shift exponent λ is equal to the reciprocal of the critical length exponent. Renormalization equations are used for the first time to calculate the heat capacity of the three-dimensional Ising model over a wide temperature range. In addition, the effect of surface anisotropy is considered for ferromagnetic strips, and procedures are outlined for obtaining analytic derivatives of the free energy with respect to the renormalized parameters.

I. INTRODUCTION

The renormalization-group concepts introduced by Kadanoff[1] and Wilson[2] have resulted in great progress in the study of critical phenomena. Applications of these ideas have utilized either a perturbation expansion in momentum space,[2] or a coarse-graining method in real space. However, either approach requires the symmetry of the underlying lattice to remain unchanged after any number of renormalization transformations, which implies that the lattice cannot be finite in any dimension. In this paper we present a modification of the real-space cumulant expansion method of Niemeijer and Van Leeuwen[3] so as to permit calculations on bounded systems.[4]

The modified cumulant expansion technique is illustrated for ferromagnetic Ising strips on a square lattice infinite in one dimension and ferromagnetic Ising slabs on a cubic lattice infinite in two dimensions. The results of our calculations are carefully examined in order to determine the limitations and successes of the method. Our calculations can be easily extended to other systems and different kinds of boundary conditions.

Section II reviews the cumulant expansion method and Sec. III presents the modifications required for the case of a finite thickness in one dimension. Renormalization equations are derived, as an example, for the first-order cumulant expansion on the square lattice. In the Appendix we give a general analysis for any order in the cumulant expansion to determine the number of interaction parameters for a Hamiltonian that will preserve the form of the surface interactions upon renormalization. In Sec. IV we review briefly the transfer matrix method[5] of obtaining exact results for very thin ferromagnetic strips, and in Sec. V we obtain the heat-capacity and magnetization curves for a first-order cumulant expansion calculation on ferromagnetic strips, with cell sizes of four and nine spins. In the same section we give the results of a second-order calculation with a cell of four spins, and we compare with the exact results from the transfer matrix method. We carry out calculations for the Ising system on a simple cubic lattice using the first-order cumulant expansion with an eight-spin cell, and we determine the shift of the critical temperature with changing thickness. We find good agreement with the proposed scaling law of Fisher and Barber.[6] Finally in Sec. V we investigate the effects of surface anisotropy[7] in the coupling between spins for ferromagnetic strips. The conclusions are presented in Sec. VI.

In the Appendix we give the expressions for the analytic derivatives of the free energy with respect to the renormalized parameters which are required to obtain accurate magnetization and heat-capacity curves near the critical point.

II. CUMULANT EXPANSION

In the cumulant expansion method of Niemeijer and Van Leeuwen[4] the system is divided into groups of spins (cells), and a renormalization transformation is defined to convert the starting Hamiltonian into one in which every cell has been replaced by a single spin. The new Hamiltonian can be expanded in terms of averages weighted by the intracell energies, giving the parameters for the new Hamiltonian in

 ©1980 The American Physical Society

terms of those for the old. In this paper the cumulant expansion method is modified for nearest-neighbor Ising Hamiltonians describing systems of thickness $L=(n-1)a$ (where a is the lattice spacing and n is the number of spin sites perpendicular to the surface) in one dimension, and infinite in the remaining d dimensions ($d=1,2$). We shall refer to these as ferromagnetic strips and slabs, respectively.

The real-space renormalization transformation proceeds as follows. We group the spins of our system into cells of b^{d+1} spins, forming a new lattice of the same symmetry, but with spacing $a'=ba$ and thickness $L'=(n/b-1)a'$. Thus the number of layers in the system has shrunk by a factor of b. We now replace each cell by a single new spin interacting with new nearest-neighbor and magnetic field coupling parameters, such that the form of the Hamiltonian and the value of the partition function are preserved. Repeated transformations reduce the number of layers in the finite dimension, until it collapses into a system of dimensionality d. The slabs collapse into the 2D (two-dimensional) Ising model and the strips into the 1D Ising model, both of which can be solved. For a system of cell size b^{d+1} and thickness $a(b^t-1)$, the renormalization transformation must be repeated t times in order to reach the lower dimensionality. The free energy of the original system can be related to that of the collapsed system by relating the new coupling parameters to the old at each step in the process.

We use a nonlinear renormalization transformation of the form

$$\exp\left[\frac{-\mathcal{H}'\{\sigma'\}}{k_BT}\right]=\sum_{\{\sigma\}}\prod_j \tfrac{1}{2}[1+\sigma_j'\,\mathrm{sgn}(j\text{th cell})]\exp\left[\frac{-\mathcal{H}\{\sigma\}}{k_BT}\right], \tag{1}$$

where k_B is Boltzmann's constant and the sign of the spin of each cell is determined by a modified majority spin rule described below. Equation (1) has the effect of scaling the free energy per spin F by a factor b^{-d-1}, i.e.,

$$-F/k_BT=\frac{1}{N}\ln\left[\sum_{\{\sigma\}}\exp(-\mathcal{H}\{\sigma\}/k_BT)\right]=b^{-d-1}F'/k_BT\ . \tag{2}$$

If we split the original Hamiltonian into two parts

$$\mathcal{H}\{\sigma\}=\mathcal{H}_0\{\sigma\}+V\{\sigma\}\ , \tag{3}$$

where $\mathcal{H}_0\{\sigma\}$ contains any constant terms, the magnetic field terms, and all couplings within cells, while $V\{\sigma\}$ contains all couplings between cells, then we can express the transformation in terms of averages weighted by the cell Hamiltonian $\mathcal{H}_0$ of the general form

$$\langle A\rangle_0=\frac{\sum_{\{\sigma\}}\prod_j[1+\sigma_j'\,\mathrm{sgn}(j\text{th cell})]\exp(-\mathcal{H}_0\{\sigma\}/k_BT)A\{\sigma\}}{\sum_{\{\sigma\}}\prod_j[1+\sigma_j'\,\mathrm{sgn}(j\text{th cell})]\exp(-\mathcal{H}_0\{\sigma\}/k_BT)}\ . \tag{4}$$

Taking the logarithm of Eq. (1) and expanding in powers of V one arrives at the cumulant expansion

$$\mathcal{H}'\{\sigma'\}=-k_BT\sum_j\ln\left[\sum_{\{\sigma\}}\tfrac{1}{2}[1+\sigma_j'\,\mathrm{sgn}(j\text{th cell})]\exp(-\mathcal{H}_0\{\sigma\}/k_BT)\right]-\langle V\rangle_0-(\langle V^2\rangle_0-\langle V\rangle_0^2)/2K_BT-(\langle V^3\rangle_0-3\langle V\rangle_0\langle V^2\rangle_0+2\langle V\rangle_0^3)/6k_B^2T^2+\cdots\ . \tag{5}$$

The new Hamiltonian is determined to the desired order in J/k_BT (J is the nearest-neighbor coupling) by truncating this series and evaluating the required averages. The cell spins are assigned by a majority spin rule, modified so that if there is a net spin of zero, the configuration is assigned half to a positive cell spin and half to a negative cell spin. We found that this majority spin rule gives better results for the critical point and critical exponents than the spin assignment used by Niemeijer and Van Leeuwen.[3]

With the cumulant expansion method, we have choices in defining the size of the cell and the order of the expansion. The effects of both of these factors will be studied by comparing the renormalization-transformation results to exact results wherever possible.

III. RENORMALIZATION EQUATIONS FOR FERROMAGNETIC STRIPS AND SLABS

We consider a nearest-neighbor Ising model on a square lattice $[\infty\times(n-1)a]$ and on a simple cubic lattice $[\infty\times\infty\times(n-1)a]$ with free-surface boundary conditions. In this case the system simply stops at the surface and the first and nth planes (or rows)

of spins are coupled to only one adjacent layer. The Hamiltonian is of the form

$$\mathcal{H}\{\sigma\} = -J \sum_{\langle i,j \rangle} \sigma_i \sigma_j - H \sum_i \sigma_i + g \ , \tag{6}$$

where J is the coupling between nearest-neighbor spins σ_i, σ_j of magnitude ± 1, H is the external magnetic field, and g a constant. The first sum runs over all nearest-neighbor pairs of lattice sites $\langle i,j \rangle$.

As discussed in the previous section, grouping the spins into cells divides the Hamiltonian into interactions within cells $\mathcal{H}_0$ and between cells V. The presence of a free surface alters the intercell potential V and gives rise to a set of coupling constants different from the bulk, describing spin interactions near the surface. The number of planes of spins that are affected by the surface depends on the dimensionality and cell size, as well as the order of the cumulant expansion. In the Appendix we show how the number of spins affected by the surface can be determined in general. In this section we use the ferromagnetic strip ($d=1$) as an example and show how the free-surface boundary conditions can be introduced in the first-order cumulant expansion with a cell of four spins.

In this case the bulk spins begin in the third layer, and a total of eight parameters are required to define the new Hamiltonian: three nearest-neighbor coupling parameters, three field parameters, and two spin-independent parameters. Figure 1 shows the transformation for the first-order cumulant expansion with four-spin cells on the square lattice. Each cell spin experiences a renormalized field that depends on the number and nature of the interactions involving the spins constituting that cell. In the bulk (two or more lattice bonds from the surface) the spins have a coupling J_B and a magnetic field H_B, and give rise to the same J_B' and H_B' for all bulk cells. Surface cells, however, have fewer interactions and experience a different renormalized field, H_1', than bulk cells. The contributions to $\langle V \rangle_0$ from surface cells are therefore

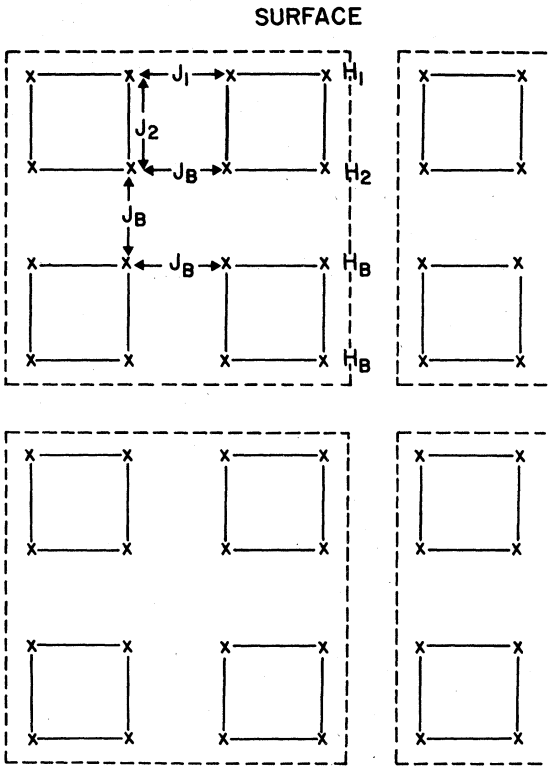

FIG. 1. Coupling parameters for four-spin cell in first-order cumulant expansion.

different than for bulk cells, and this results in a different renormalized field, H_2', on the cells next to the surface, as well as a different nearest-neighbor coupling between surface cells J_1' and between surface cells and next-to-surface cells J_2'. Furthermore, since averages over each cell contribute a constant term to the new Hamiltonian, there will be one spin-independent parameter, g_B', arising from the bulk cells, and a second, g_S', arising from the surface cells. The Hamiltonian then takes the form

$$\mathcal{H}\{\sigma\} = \tfrac{1}{4} \sum_{\langle i \rangle_{S,NS}} g_S + \tfrac{1}{4} \sum_{\langle i \rangle_B} g_B - H_1 \sum_{\langle i \rangle_S} \sigma_i - H_2 \sum_{\langle i \rangle_{NS}} \sigma_i$$
$$- H_B \sum_{\langle i \rangle_B} \sigma_i - J_1 \sum_{\langle i,j \rangle_{\parallel}} \sigma_i \sigma_j - J_2 \sum_{\langle i,j \rangle_{\perp}} \sigma_i \sigma_j - J_B \sum_{\langle i,j \rangle_B} \sigma_i \sigma_j - J_B \sum_{\langle i,j \rangle_{\perp NS}} \sigma_i \sigma_j - J_B \sum_{\langle i,j \rangle_{NS}} \sigma_i \sigma_j \ , \tag{7}$$

where $\langle i \rangle_S$ denotes a summation over surface spins, $\langle i \rangle_{NS}$ over spins next to the surface, $\langle i \rangle_B$ over bulk spins, $\langle i,j \rangle_{\parallel}$ over nearest neighbors on the surface, $\langle ij \rangle_{\perp}$ over nearest neighbors with one spin on the surface and one spin next to the surface, $\langle i,j \rangle_B$ over nearest neighbors in the bulk, $\langle i,j \rangle_{\perp NS}$ over nearest neighbors with one spin in the second and one in the third layers, and $\langle i,j \rangle_{NS}$ over nearest neighbors both next to the surface. When we divide the Hamiltonian into inter- and intracell parts we obtain

$$\mathcal{H}\{\sigma\} = \sum_{\substack{\text{surface} \\ \text{cells}}} \mathcal{H}_0\{\sigma\}_S + \sum_{\substack{\text{bulk} \\ \text{cells}}} \mathcal{H}_0\{\sigma\}_B + V\{\sigma\} \ , \tag{8}$$

with

$$\mathcal{H}_0\{\sigma\}_S = g_S - H_1 \sum_{\langle i \rangle_S} \sigma_i - H_2 \sum_{\langle i \rangle_{NS}} \sigma_i - J_1 \sum_{\langle i,j \rangle_{\parallel}} \sigma_i \sigma_j$$
$$- J_2 \sum_{\langle i,j \rangle_{\perp}} \sigma_i \sigma_j - J_B \sum_{\langle i,j \rangle_{NS}} \sigma_i \sigma_j \tag{9}$$

and

$$\mathcal{H}_0\{\sigma\}_B = g_B - H_B \sum_i \sigma_i - J_B \sum_{\langle i,j\rangle_B} \sigma_i\sigma_j \ , \tag{10}$$

where all sums are over spins within the cell, and

$$V\{\sigma\} = -J_1 \sum_{\langle i,j\rangle_{\parallel}} \sigma_i\sigma_j - J_B \sum_{\langle i,j\rangle_B} \sigma_i\sigma_j - J_B \sum_{\langle i,j\rangle_{NS}} \sigma_i\sigma_j - J_B \sum_{\langle i,j\rangle_{\perp NS}} \sigma_i\sigma_j \ , \tag{11}$$

where all sums are restricted to pairs of spins between cells. With these definitions of V and H_0, Eq. (5) gives rise to terms in the new Hamiltonian $\mathcal{H}'$ that represent new field and nearest-neighbor coupling terms. To first order in J/k_BT, with the summations now over the new spins $\langle\sigma'\rangle$, we find

$$\begin{aligned}\mathcal{H}'\{\sigma'\} = &\sum_{\langle i\rangle_S} [g_S - \tfrac{1}{2}(1+\sigma_i')\ln Z_S - \tfrac{1}{2}(1-\sigma_i')\ln Z_{-S}] + \sum_{\langle i\rangle_{NS,B}} [g_B - \tfrac{1}{2}(1+\sigma_i')\ln Z_B - \tfrac{1}{2}(1-\sigma_i')\ln Z_{-B}] \\ &+ \sum_{\langle i,j\rangle_{\parallel}} [J_1(a_{-1}+\sigma_i' a_1)(a_{-1}+\sigma_j' a_1) + J_B(a_{-2}+\sigma_i' a_2)(a_{-2}+\sigma_j' a_2)] \\ &+ 2J_B \sum_{\langle i,j\rangle_{\perp}} (a_{-2}+\sigma_i' a_2)(a_{-B}+\sigma_j' a_B) + 2J_B \sum_{\langle i,j\rangle_{NS,\perp NS,B}} (a_{-B}+\sigma_i' a_B)(a_{-B}+\sigma_j' a_B) \ ,\end{aligned} \tag{12}$$

where

$$\begin{aligned} a_{\pm i} &= \tfrac{1}{2}(C_i/Z_S \mp C_{-i}/Z_{-S}), \quad i=1,2 \ , \\ a_{\pm B} &= \tfrac{1}{2}(C_B/Z_B \mp C_{-B}/Z_{-B}) \ ,\end{aligned} \tag{13}$$

and

$$\begin{aligned} Z_{\pm S} = &\exp[(J_1+2J_2+J_B \pm 2H_1 \pm 2H_2)/k_BT] + 2\exp[(-J_1+J_B \pm 2H_2)/k_BT] + 2\exp[(J_1-J_B \pm 2H_1)/k_BT] \\ &+ \exp[(J_1-2J_2+J_B)/k_BT]\cosh[(\pm 2H_1 \mp 2H_2)/k_BT] + 2\exp[(-J_1-J_B)/k_BT]\cosh(2J_2/k_BT) \ , \end{aligned} \tag{14}$$

$$Z_{\pm B} = \exp[4(J_B \pm H_B)/k_BT] + 4\exp(\pm 2H_B/k_BT) + 2 + \exp(-4J_B/k_BT) \ , \tag{15}$$

$$\begin{aligned} C_{\pm i} = \pm\{ &\exp[(J_1+2J_2+J_B \pm 2H_1 \pm 2H_2)/k_BT] + 2\exp[(-1)^i(J_B-J_1)/k_BT \pm 2H_i/k_BT] \\ &+ (-1)^i \exp[(J_1-2J_2+J_B)/k_BT]\sinh[(\mp 2H_1 \pm 2H_2)/k_BT]\}, \quad i=1,2 \ , \end{aligned} \tag{16}$$

$$C_{\pm B} = \pm\{\exp[4(J_B \pm H_B)/k_BT] + 2\exp(\pm 2H_B/k_BT)\} \ . \tag{17}$$

Rearranging Eq. (12) into the form of Eq. (7), we arrive at the following set of renormalization equations[8]:

$$\begin{aligned} g_S' &= 2g_S + 2g_B - 2J_1 a_{-1}^2 - 2J_B a_{-2}^2 - 4J_B a_{-2}a_{-B} - 6J_B a_{-B}^2 - \ln(Z_S Z_{-S} Z_B Z_{-B}) \ , \\ g_B' &= 4g_B - 16J_B a_{-B}^2 - 2\ln(Z_B Z_{-B}) \ , \\ H_1' &= 2J_1 a_1 a_{-1} + 2J_B a_2 a_{-2} + 2J_B a_2 a_{-B} + \tfrac{1}{2}\ln(Z_S/Z_{-S}) \ , \\ H_2' &= 6J_B a_B a_{-B} + 2J_B a_B a_{-2} + \tfrac{1}{2}\ln(Z_B/Z_{-B}) \ , \\ H_B' &= 8J_B a_B a_{-B} + \tfrac{1}{2}\ln(Z_B/Z_{-B}) \ , \\ J_1' &= J_1 a_1^2 + J_B a_2^2; \quad J_2' = 2J_B a_2 a_B; \quad J_B' = 2J_B a_B^2 \ . \end{aligned} \tag{18}$$

When we reach a thickness corresponding to four rows, we have only surface cells and the bulk field and spin-independent parameters do not appear in the Hamiltonian. A further reduction of the thickness produces only surface spins, and we obtain a new set of renormalization equations,

$$\begin{aligned} \hat{g}_S &= 4g_S - 4J_1 a_{-1}^2 - 8J_B a_{-2}^2 - 2\ln(Z_S Z_{-S}) \ , \\ \hat{H}_1 &= \hat{H}_2 = 2J_1 a_1 a_{-1} + 4J_B a_2 a_{-2} + \tfrac{1}{2}\ln(Z_S/Z_{-S}) \ , \\ \hat{J}_1 &= \hat{J}_B = J_1 a_1^2 + J_B a_2^2 \ , \\ \hat{J}_2 &= 2J_B a_2^2 \ , \end{aligned} \tag{19}$$

where $a_{\pm i}$, $Z_{\pm S}$ are given by Eqs. (13) and (14). We now have only four parameters describing a one-dimensional array of cells. The final transformation into the one-dimensional Ising model is given by

$$\begin{aligned} g^* &= \hat{g}_S - 2\hat{J}_1 a_{-1}^2 - \tfrac{1}{2}\ln(\hat{Z}_S \hat{Z}_{-S}) \ , \\ H^* &= 4\hat{J}_1 a_1 a_{-1} + \tfrac{1}{2}\ln(\hat{Z}_S/\hat{Z}_{-S}) \ , \\ J^* &= 2\hat{J}_1 a_1^2 \ , \end{aligned} \tag{20}$$

where now

$$\begin{aligned} \hat{Z}_{\pm S} = &\exp[2(\hat{J}_1 + \hat{J}_2 \pm 4\hat{H}_1)/k_B T] \\ &+ 4\exp(\pm 2\hat{H}_1/k_B T) \\ &+ 2\cosh[2(\hat{J}_1 - \hat{J}_2)/k_B T] \\ &+ \exp[-2(\hat{J}_1 + \hat{J}_2)/k_B T] \ , \end{aligned} \tag{21}$$

and $a_{\pm 1}$ are given by Eq. (13), with $C_{\pm 1}$ replaced by

$$\begin{aligned} \hat{C}_{\pm 1} = \pm\{ &\exp[2(\hat{J}_1 + \hat{J}_2 \pm 4\hat{H}_1)/k_B T] \\ &+ 2\exp(\pm 2\hat{H}_1/k_B T)\} \ . \end{aligned} \tag{22}$$

To summarize, for a system of thickness $a(b^t - 1)$, after t successive renormalizations we arrive at a one-dimensional Ising model with parameters $g^*(t)$, $H^*(t)$, and $J^*(t)$, where the asterisk denotes the lower dimensionality. These parameters are defined in terms of the parameters of the original system. The free energy (per spin) of the collapsed system is then related to that of the original system by repeated use of Eq. (2), thus

$$\begin{aligned} &F(b^t; g_B, H_B, J_B, g_S, H_1, H_2, J_1, J_2) \\ &\qquad = b^{-t} F(1; g^*, H^*, J^*) \ . \end{aligned} \tag{23}$$

Usually $g_S = g_B = 0$, $H_1 = H_2 = H_B$, and $J_1 = J_2 = J_B$ initially but it is not necessary to restrict ourselves to this case.

A similar procedure can be followed to derive equations for the second-order cumulant expansion with four spins per cell, and the first-order expansion with nine spins per cell. We have also derived the renormalization equations for the first-order expansion with eight spins per cell for the simple cubic lattice.

In Sec. V we give the results of calculations of the free energy, its derivative with respect to $J/k_B T$, and the heat capacity, as well as the magnetization as a function of temperature, field strength, and thickness. Also included in our calculations is the effect of a surface coupling different from the bulk on the heat capacity. In the Appendix we give general formulas for relating the derivatives of the free energy of the original system to derivatives, with respect to renormalized parameters, of the free energy of the collapsed system. The use of analytic derivatives is essential near the fixed point corresponding to the infinite $(d+1)$ dimensional system because numerical techniques fail when the distance from the fixed point becomes less than the size of the numerical increment. As there are limits to the increment size, due to computational round-off errors, it is necessary to use the procedure outlined in the Appendix to determine derivatives near the fixed point accurately.

IV. TRANSFER MATRIX TECHNIQUE FOR THIN STRIPS

For the application of the transfer matrix technique[5] we consider the strip to consist of m columns of n spins each, such that a particular column, the jth for example, interacts only with the $(j-1)$th and $(j+1)$th column. Following Newell and Montroll,[5] we write the energy of this system in the form

$$V = \sum_{j=1}^{m-1} V(\nu_j, \nu_{j+1}) + \sum_{j=1}^{m} V(\nu_j) \ , \tag{24}$$

where $V(\nu_j, \nu_{j+1})$ is the interaction energy between the jth and $(j+1)$th columns, and $V(\nu_j)$ is the internal energy of the jth column. The quantity ν_j denotes the set of all internal coordinates of the jth column.

Introducing periodic boundary conditions so that the mth column is connected to the first, the partition function of the system is given by

$$Z = \sum_{\nu_1} \cdots \sum_{\nu_m} \prod_{j=1}^{m} \underline{P}(\nu_j, \nu_j + 1) \ , \tag{25}$$

where

$$\underline{P}(\nu_j, \nu_{j+1}) = \exp\{-[V(\nu_j, \nu_{j+1}) + V(\nu_j)]/k_B T\} \tag{26}$$

is an element of a matrix $\underline{P}$. Clearly

$$Z = \mathrm{trace}(\underline{P}^m) = \sum_j \lambda_j^m \ , \tag{27}$$

where $\{\lambda_j\}$ is the set of characteristic values of the matrix $\underline{P}$. Finally, for a very large system we get

$$\lim_{m\to\infty} m^{-1} \ln Z = \ln \lambda_{\max} \tag{28}$$

and the problem reduces to finding the largest eigenvalue of the transfer matrix $\underline{P}$. The numerical computation of this eigenvalue was carried out for the two-dimensional ferromagnetic strips using the method of Lewis.[9] In practice it appears that the transfer matrix method becomes impractical for $n > 10$, as the size of the matrix grows rapidly. The results of the calculation for $n = 8$ are shown in Fig. 2.

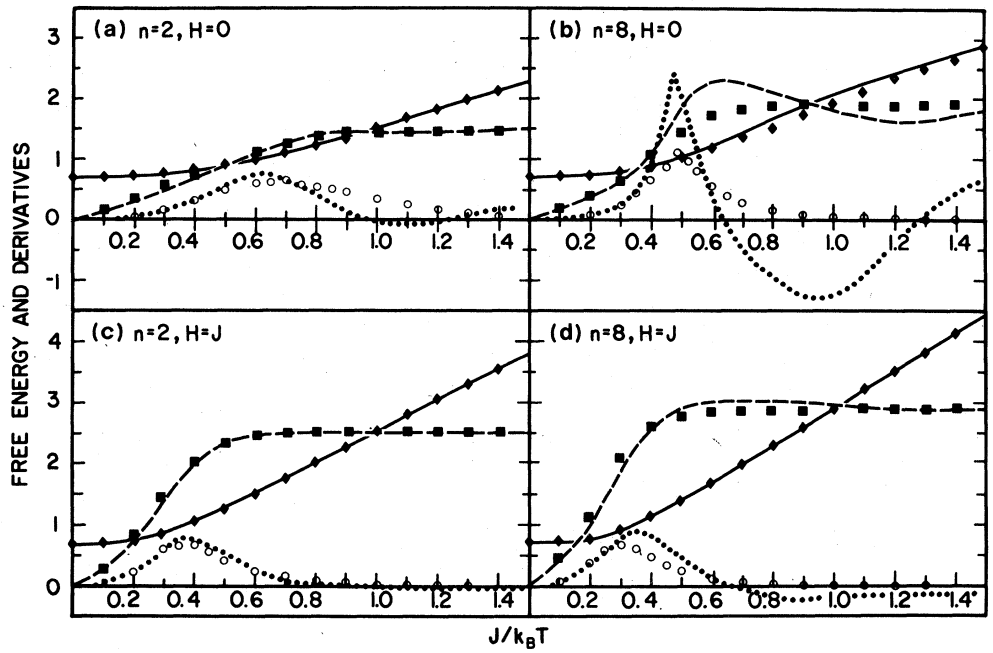

FIG. 2. Free energy per spin $(-F/k_BT)$ (−▲−▲−▲−), $\partial(-F/k_BT)/\partial(J/k_BT)$ (−■−■−■−), and C_v/Nk_B(···○···○···) vs J/k_BT for ferromagnetic strips of dimension $[\infty \times (n-1)a]$. The lines and the various symbols represent the renormalization-group calculations and the transfer matrix calculations, respectively. (a) $n=2$, $H=0$; second-order cumulant and four-spin cell. (b) $n=8$, $H=0$; second-order cumulant and four-spin cell. (c) $n=2$, $H=J$; first-order cumulant and four-spin cell. (d) $n=8$, $H=J$; first-order cumulant and four-spin cell.

V. RESULTS AND DISCUSSION

A. Thin ferromagnetic strips ($1 \leq n \leq 9$)

For small n, we have obtained the free energy and its derivatives using the transfer matrix technique described in the previous section and we compare the renormalization-group calculations to these exact results as shown in Fig. 2. Figure 2(a) shows the free energy, first derivative, and heat capacity for a two-layer (thickness a) Ising strip in the absence of a magnetic field. The agreement of the second-order cumulant expansion and a four-spin cell with the exact result is very good, although the heat capacity peaks too soon and falls too rapidly. Figure 2(b) shows the results for a strip of thickness $7a$ ($n=8$). Here there is good agreement with the exact free energy, but the first derivative demonstrates a severe overshoot above the pseudocritical point, the heat-capacity peak is too high and the heat capacity becomes *negative* over a wide range of J/k_BT.

The overshoot of the first derivative and the negative heat capacity can be understood as follows. Using Eq. (4), it can be shown that the cumulant averages in Eq. (5) all vanish in the limit $T=0$. Hence we obtain the correct free energy in this limit for any order of the cumulant expansion. As the expansion is explicitly in powers of T^{-1}, and the cumulant averages, hence the coefficients of the series, are bounded, we also obtain the correct high-temperature behavior of the free energy. At intermediate temperatures Fig. 2(b) indicates that the approximate (negative) free energy falls too rapidly as the temperature increases up to the pseudocritical point. Beyond this point, in order to reach the correct high-temperature limit, there is a resulting overshoot in the first derivative and a region of negative heat capacity corresponding to the negative curvature in the free energy.

Physically the initial rapid decrease of the free energy with increasing temperature arises from the truncation of the cumulant expansion resulting in a neglect of correlations in the renormalization transformation. For example, close to $T=0$, use of the majority spin rule leads upon transformation to the loss of the few spin deviations (inverted spins) which are present in the system, and thus to a sum inside the free energy expression, Eq. (2), which is *greater* than if the spin deviations were retained. This overestimate persists until near the pseudocritical point, when there is a large number of spin deviations and the majority spin rule gives a better description of the spin correlations in the renormalization transformation.

From the above discussion the overshoot effect may be expected to be larger in two dimensions than

in one dimension and this trend is evident from the results for the thicker strip in a comparison of Figs. 2(a) and 2(b). Later we will see that for three dimensions the relative error in the approximate free energy is even larger. The approximation is greatly improved however by the presence of an external magnetic field, as shown in Figs. 2(c) and 2(d). At low temperatures and with an external magnetic field the relative error in the approximate free energy resulting from the neglect of spin deviations in the renormalization transformation is smaller than before, and since the high-temperature limit of the free energy is given correctly, the agreement with the exact results is improved over the whole temperature range. The agreement between the renormalization approximation and the exact free energy is excellent in Fig. 2(c), and in Fig. 2(d) the approximation is very good, showing a smaller negative heat capacity than in Fig. 2(b).

B. Thick ferromagnetic strips and slabs ($n \to \infty$)

Because we are working with finite lattices, the renormalization produces a system composed of a different number of layers with each transformation, and there is no true fixed point. However for $n \gtrsim 64$ we rapidly approach the case of an infinite system. In Fig. 3 we show the approximate heat capacity as a function of the reciprocal temperature for very thick ferromagnetic strips ($n = 2^9$ for four-spin cells, $n = 3^6$ for nine-spin cells), along with the exact Onsager result for the two-dimensional Ising model.[10] As in the case of thin strips, a striking feature is the region of negative heat capacity. The reason for this behavior has been discussed in the previous subsection. Here we make the added observation that the area under the specific-heat curve can be related to the entropy, which is given correctly in the high-temperature limit in our calculations. From Fig. 3 we see that the positive area, for a given expansion order and cell size is in general greater than the area under the curve corresponding to the exact result. Hence the region of negative specific heat is necessary to partly cancel the effect of the positive part, and to give the entropy correctly in the high-temperature limit.

As seen from Fig. 3 the second-order cumulant expansion with a four-spin cell gives the best results for the specific heat on the high-temperature side of the singularity, while on the low-temperature side the approximate specific heat falls too slowly and becomes negative. Both first-order results (with four-spin and nine-spin cells) give similar disagreement with respect to the shape of the curve, and also show a larger shift of the maximum from the two-dimensional critical point.

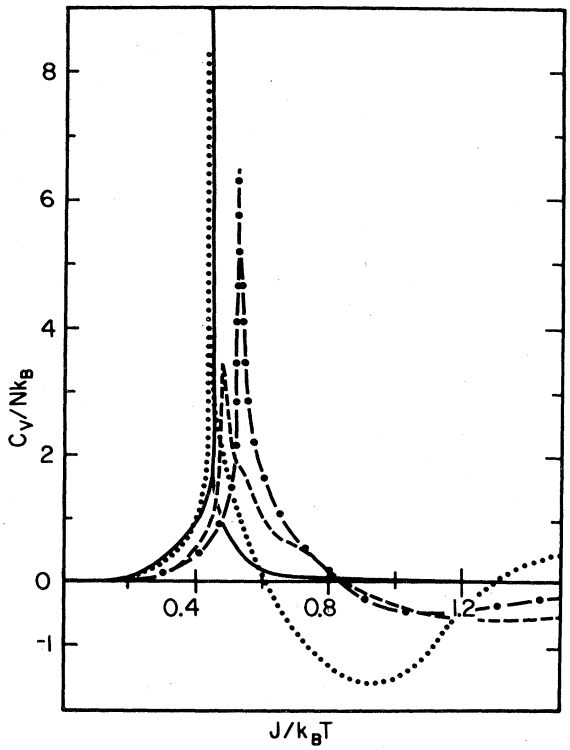

FIG. 3. Heat capacity C_v/Nk_B of ferromagnetic strips $[\infty \times (n-1)a]$ vs J/k_BT for first-order cumulant and four-spin cell with $n = 2^9$ (—●—●—), first-order cumulant and nine-spin cell with $n = 3^6$ (— — —), second-order cumulant and four-spin cell with $n = 2^9$ (···), exact result for $n = \infty$ (——).

We may check the numerical accuracy of our calculations by comparing with earlier results by Hsu and Gunton[11] for an infinite two-dimensional square lattice. Table I shows our results for the two-dimensional system. We have determined the fixed-point solutions as well as the magnetic and thermal eigenvalues to a greater degree of accuracy than previously. In particular, we have obtained the fixed-point solution to six significant figures, and computed

TABLE I. Two-dimensional results for y_T, y_H, and J_c/k_BT_c for 2×2 and 3×3 cells on a square lattice.

Cell Size	Order of cumulant expansion	y_T	y_H	J_c/k_BT_c
2×2	1	1.005 90	2.145 90	0.518 612
	2	1.029 13	1.999 15	0.430 197
3×3	1	0.927 04	1.943 31	0.469 742
Exact		1.0	1.875	0.440 687

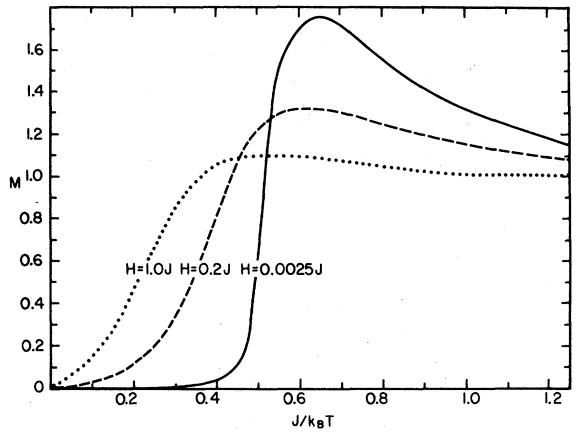

FIG. 4. Magnetization M (dimensionless) vs J/k_BT for various values of H/J.

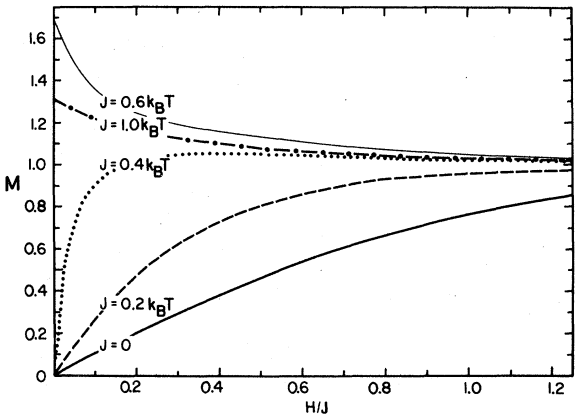

FIG. 5. Magnetization M (dimensionless) vs H/J for constant temperature and fixed values of J/k_BT.

the eigenvalues from a matrix consisting of *algebraic* expressions (given in the Appendix) for derivatives with respect to the field and coupling parameters. Except for the second-order four-spin cell results, the values of Hsu and Gunton[11] are in agreement with ours.

Figure 4 shows the magnetization $M=-\partial(F/k_BT)/\partial(H/k_BT)$ vs J/k_BT at different field strengths for a first-order cumulant expansion with a four-spin cell. From the exact result, $M=\mathrm{sgn}H$ for $T\to 0$, we see that the magnetization is bounded by unity, whereas the calculated value rises above this value as the temperature is increased, and shows a large overshoot in the critical region before falling at high temperature. The explanation of this effect is similar to that given in Sec. V A for the anomalous behavior of the heat capacity. The neglect of spin correlations in the renormalization transformation at low temperatures gives rise to an overestimate of the magnitude of the free energy, which however is given correctly in the high-temperature limit. The anomalous behavior of the derivatives in the critical region corresponds to the regime where the free energy is changing towards its correct value. As expected, the renormalization transformation gives a better approximation at higher fields and the overshoot effect is decreased. Comparing our results with the cluster approximation of Nienhuis and Nauenberg,[12] we see that there is good agreemet over the whole temperature range for $H=J$, and over the high-temperature region for the other H values. It is interesting to note that the cluster approximation does not give rise to the overshoot effect.

In Fig. 5 the magnetization is shown as a function of H/J for constant temperature and fixed values of (J/k_BT). For values less than the critical coupling J_c/k_BT_c the magnetization curves show the behavior expected for a high-temperature expansion. For greater values of the coupling parameter however, the magnetization is too large for small values of H, decaying to the correct value $M=1$ as $H\to\infty$. Again, this effect arises from the overordering of the spins at low temperature, inherent in our renormalization transformation.

Figure 6 shows the approximate heat capacity calculated for a ferromagnetic slab $[\infty\times\infty\times(n-1)a]$ with $n=64$ using a first-order cumulant expansion and an eight-spin cell. The values shown are very close to the results obtained with the first-order expansion for $n=\infty$. Also shown is the extrapolation from high- and low-temperature series expansions.[13–15] It is evident that we do not obtain a good

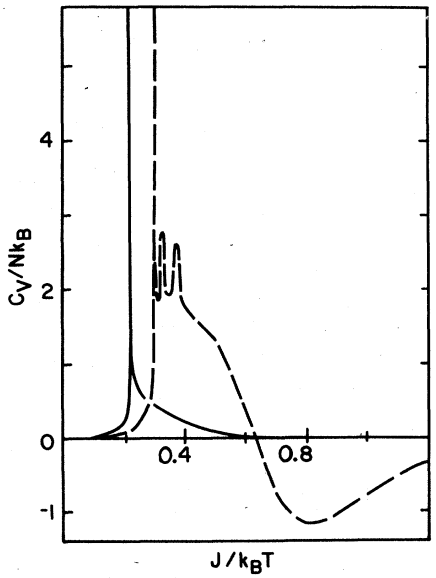

FIG. 6. Heat capacity C_v/Nk_B of ferromagnetic slabs $[\infty\times\infty\times(n-1)a]$ with first-order cumulant expansion and eight-spin cell on a simple cubic lattice, $n=64$ (– – –), and extrapolations of series expansions (high and low temperature) (——).

approximation to the three-dimensional critical point ($J_c/k_BT_c = 0.2217$) in this case. In addition to the negative heat-capacity region found earlier for ferromagnetic strips, there are oscillations in the heat capacity for the coupling parameter just above the singularity. The oscillations arise because of the coarse graining of the system by the grouping of spins into cells, and they are more severe in the case of a slab than for a strip because of the different power-law dependence of the correlation length on the deviation from the critical temperature in the two cases. For a two-dimensional Ising model the correlation length ξ varies as $|T_c - T|^{-1}$ near the critical temperature, whereas for the three-dimensional case we have $\xi \propto |T_c - T|^{-0.64}$ (Ref. 16). For a ferromagnetic slab the correlation length grows more slowly than in two dimensions, and is large but finite over a wider temperature range. Hence in this case, changes in the free energy are more sensitive to the coarse graining in the renormalization transformation. The effect is particularly noticeable in the ferromagnetic phase, because the spins in the cells are almost entirely aligned, and are included in the free energy as discrete units, whereas in the paramagnetic phase the average cell spin is much smaller, and the effect of discretization is negligible.

C. Ferromagnetic strips and slabs of intermediate thickness ($10 \leq n \leq 1000$)

The properties of the ferromagnetic strips and slabs approach, with increasing thickness, the bulk properties. In this section we examine the rate at which the bulk properties are approached. As an example, plots of the heat capacity versus temperature for the Ising strip show a distinct maximum (pseudocritical point) which with increasing strip width becomes sharper and is shifted closer to the critical point of the two-dimensional Ising model. Similarly, for magnetic slabs we see the singularity in the heat capacity occurring, with increasing thickness, nearer to the critical point of the three-dimensional Ising model.

The shift of the singularity for the magnetic slabs can be expressed by a power-law dependence, from the following argument. As the transformation equations for the Hamiltonian parameters are smooth and continuous, any singularity in the $(d+1)$-dimensional system must arise from the singularity existing in the d-dimensional system related to it by Eq. (13). The value of the coupling for $n = b^t$ layers, $K_c(n) = J/k_BT_c$, will then be related to $K_c^d(\infty)$ by t successive applications of the renormalization transform. Similarly $K_c(n-1)$ will be related to $K_c^d(\infty)$ by $t-1$ transformations. Clearly

$$K_c(n-1) = K'[K_c(n)] \ . \tag{29}$$

For systems sufficiently thick, $K_c(n)$, $K_c(n-1)$ will be near the fixed point of the infinite $(d+1)$-dimensional lattice. This allows use of the linear relationship

$$K_c(n-1) = K'[K_c(n)] \approx K_c^{d+1}(\infty) + b^{1/\nu}[K_c(n) - K_c^{d+1}(\infty)] \ , \tag{30}$$

thus

$$[K_c(n) - K_c^{d+1}(\infty)] \approx b^{-1/\nu}[K_c(n-1) - K_c^{d+1}(\infty)] \propto b^{-t/\nu} = n^{-1/\nu} \ . \tag{31}$$

Since $K \equiv J/k_BT$, we can write Eq. (31) in terms of $T_c(n)$ and $T_c(\infty) = T_c^{d+1}$, rearranging to give

$$[T_c(\infty) - T_c(n)]/T_c(\infty)T_c(n) \propto n^{-1/\nu} \ . \tag{32}$$

For very large n, $T_c(n)$ approaches the constant value $T_c(\infty)$ and we recover the usual scaling result[6,17]

$$|T_c(\infty) - T_c(n)|/T_c(\infty) = Cn^{-\lambda} \ , \tag{33}$$

where λ is the shifting exponent. Thus in the limit $n \to \infty$, $\lambda = 1/\nu$.

It is better to use Eq. (32) rather than Eq. (33) because the former will approach the power-law behavior much more quickly as n increases. For this reason Eq. (32) is used for the calculations shown in Figs. 7 and 8.[18]

The derivation of Eqs. (29) to (32) for ferromagnetic strips ($d = 1$) is similar, but not as rigorous due to the occurrence of a maximum (instead of a singularity) in the heat capacity for each thickness, and the possibility that the position of the maximum in the one-dimensional system does not correspond to the value of the coupling reached after t transformations. However Eq. (33) has been verified for ferromagnetic strips by high-temperature series expansions,[19]

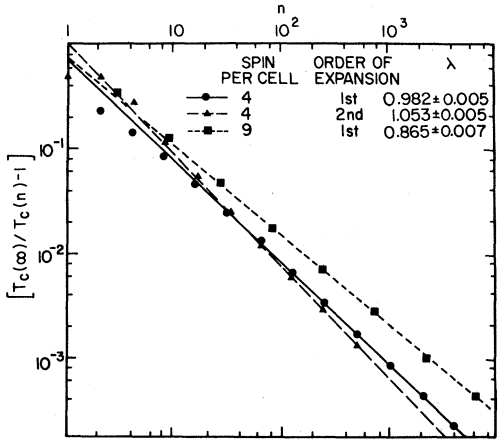

FIG. 7. Shift exponent λ for ferromagnetic strips $[\infty \times (n-1)a]$ on a square lattice, showing results of calculations using different cell sizes and orders in the cumulant expansion.

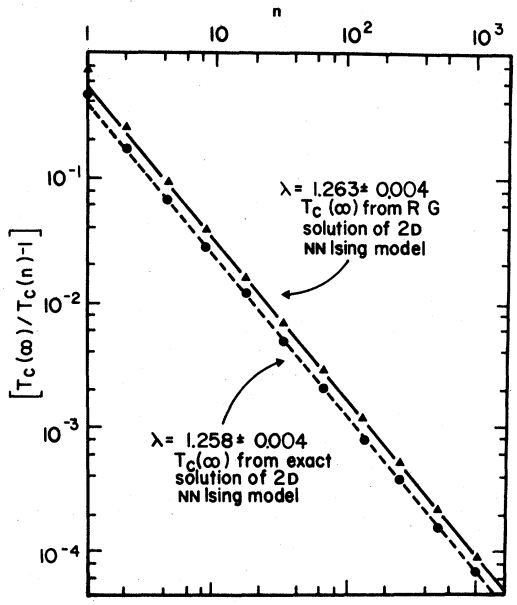

FIG. 8. Shift exponent λ for ferromagnetic slabs $[\infty \times \infty \times (n-1)a]$ on a simple cubic lattice using eight-spin cell and first-order cumulant expansion.

Monte Carlo calculations,[7] ϵ expansions,[20] and by an asymptotic ($n \to \infty$) solution for $d = 1$.[21]

Systems with constraints have lower values of λ. For example, $\lambda = 1$ for a Bose gas film[6] (where there are constant particle density constraints) and $\lambda = 1$ for a spherical model[6] (where a constant mean spin is required in a system that is not translationally invariant due to the finite system). Systems with periodic boundaries also differ from the free-surface case with $\lambda = d$ (d is the number of infinite dimensions) for $d \geq 2$, but do agree with $\lambda = 1$ for one dimension infinite.[6,17]

Figure 7 shows a log-log plot of Eq. (32) for the ferromagnetic strips. Results are shown for a first- and second-order cumulant expansion with a four-spin cell, and for a first-order expansion with a nine-spin cell. All three calculations give highly linear plots for $n > 4$, with regression correlation coefficients of better than 0.9999. This system has been studied in the asymptotic limit by Au-Yang and Fisher,[21] who arrived at $\lambda = 1$ and $C = 0.892\,785$. This agrees with our estimates of $\lambda = 0.982 \pm 0.005$, 1.053 ± 0.005, 0.865 ± 0.007, and $C = 0.724$, 1.025, 0.788 for the first-order four-spin cell, second-order four-spin cell, and first-order nine-spin cell cumulant expansions, respectively.

When the renormalization-group approximation is carried out on the ferromagnetic slabs, the resulting collapsed two-dimensional Ising model can be analyzed by either the Onsager method, or by a further renormalization approximation. In Fig. 8 we show the log-log plot of Eq. (32) where both methods have been used to study the collapsed system. The difference in the calculated shift exponents from the two methods is less than the error arising from the fitting of the lines. The value of λ found here (1.26) is less than predicted from scaling laws ($\lambda = 1.56$), Monte Carlo calculations,[7] or high-temperature series expansions.[22] However the first-order cumulant expansion, with an eight-spin cell, leads to too high a value of ν (0.803) for the infinite simple cubic lattice and in fact gives $1/\nu \sim 1.246$, which verifies the scaling relation for our system. We believe that the small difference between our values of λ and $1/\nu$ is not numerical in origin, rather it is due to insufficiently large n in Fig. 8. However there are practical limits on how large a value of n can be used, as the value of $\ln[T_c(\infty)/T_c(n)-1]$ looses one significant figure for every increase of order of magnitude in n. For $n = 1000$, we require seven significant figures in $T_c(\infty)$ and $T_c(n)$ in order to maintain three significant figures in $[T_c(\infty)/T_c(n)-1]$.

D. Surface anisotropy

We can also examine the effect of having nearest-neighbor couplings on the surface different from those in the bulk.[7] Figure 9 shows the heat capacities of eight-layer magnetic strips (thickness $7a$) for J_1/J_B ratios of 10, 5, 1, and 0.2, with $J_1 = J_2$. The results of an exact transfer matrix calculation for $J_1 = J_2 = 5J_B$ are also shown. We see the appearance of a

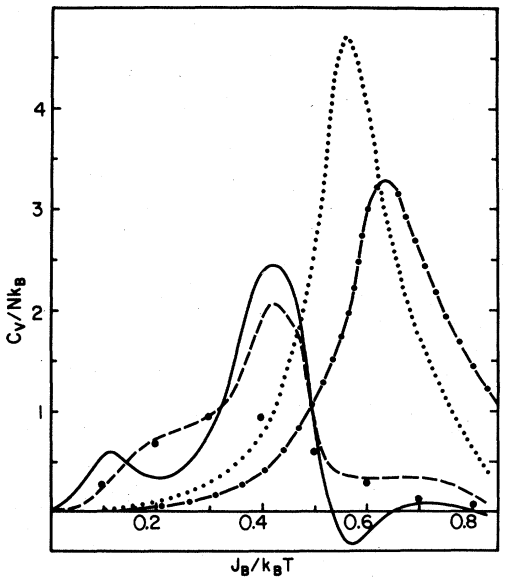

FIG. 9. Heat capacity C_v/Nk_B of a thin ferromagnetic strip ($\infty \times 8a$) with enhanced surface couplings. The results shown are for $J_1 = J_2 = 5J_B$ (– – –), $J_1 = J_2 = 0.2J_B$ (•—•—•), and $J_1 = J_2 = J_B$ (···). The transfer matrix calculations for $J_1 = J_2 = 10J_B$ (——) are shown by (●).

shoulder and then a second maximum as the relative strength of the surface coupling increases. The exact calculation shows that this effect is real and not an artifact of the renormalization transformation.

Strong surface couplings on the surface of the strip correspond to a one-dimensional cladding on a strip of smaller dimensions. The free energy per spin is higher than in the case of isotropic coupling, and the maximum in the free energy is shifted to higher temperatures. When the ratio of surface to bulk coupling is sufficiently high, the heat capacity can pass through a maximum for the one-dimensional Ising systems on the surface, while the bulk spins are still in a disordered state. As the temperature is lowered further the bulk spins begin to order and the heat capacity passes through a second maximum.

If the surface coupling is weak in comparison to the bulk, the maximum in the heat capacity is reduced and shifted to lower temperatures, but is insensitive to the actual ratio, the curves for $J_1 = 0.1J_B$ (not shown) and $J_1 = 0.2J_B$ being almost identical. With weak surface coupling the system behaves as if the surface layers were missing, with new dimensions $[\infty \times (n-3)a]$, and the shift of the specific-heat maximum to lower temperature corresponds to a reduction of the free energy per spin. At intermediate ratios of surface to bulk coupling there is no clear distinction between the surface and bulk contributions to the specific heat.

Since the real-space renormalization transformation does not give rise to fixed points for the finite Ising strips, surface related exponents cannot be derived for this case by our method. However the effect of surface anisotropy on the critical behavior of semi-infinite Ising models will be discussed in a forthcoming paper.[23]

VI. CONCLUSIONS

The ferromagnetic strips and slabs studied in this paper have served as good examples of the use and power of the cumulant expansion renormalization transformation for systems subject to boundary conditions. A procedure has been outlined for performing such a transformation and some of the difficulties encountered in practice for low-order cumulant expansions have been examined. A thorough discussion of these difficulties was given, and their origin in the approximate nature of the renormalization transformation was identified.

For the thin ferromagnetic strips it was possible to carry out exact calculations using the transfer matrix method in order to check the accuracy of the renormalization-group calculations. Both the Ising strips and slabs could be transformed by repeated renormalization until the system collapsed to one of lower dimensionality, where the exact temperature dependence of the thermodynamic quantities was known. Hence the results presented here in the limit of very thick slabs represent the first real-space renormalization work over the entire temperature range for three-dimensional Ising systems. These calculations have shown that the shifting exponent λ is equal to the reciprocal of the bulk correlation exponent ν as proposed by Fisher and Barber.[6]

We found that the use of analytic derivatives is essential for the calculation of the derivatives of the free energy near the fixed point. We presented general expressions for these derivatives and suggested methods of systematizing their use for computer calculations.

The method outlined in this paper allows one to introduce free-surface boundary conditions into an Ising-model renormalization-group analysis for any order of the cumulant expansion and arbitrary cell size. The method is easily extended to other systems (Heisenberg model, Potts model, percolation and polymer configuration problems), other types of surfaces (semi-infinite systems, systems finite in two or more dimensions), and other types of boundary conditions (periodic, reflecting, etc.).

ACKNOWLEDGMENTS

We would like to thank L. Marks for developing the computer program used for the transfer matrix calculations. We would also like to thank Mr. R. Cordery for showing us some of his notes on this problem, as described in Ref. 4, and A. Griffin and R. Cordery for discussions during the initial stages of this work.

APPENDIX

For a system of dimension $d+1$ we determine, as follows, the number of layers affected by the surface, and hence the number of parameters required to specify a renormalized Hamiltonian corresponding to an mth-order cumulant expansion with cell size b^{d+1}. Suppose the pth cell from the surface is the first cell composed only of bulk spins, i.e., it is dependent only on bulk spins in the renormalization transform. We proceed to determine p in terms of m and b. In the mth order of the cumulant expansion, each cell interacts with cells up to m neighboring cells distant, so that the $(p+m)$th cell is the first cell that does not interact with any surface cells and transforms into a bulk spin in the $(p+m)$th layer, this being the first layer of bulk spins. The $(p+m-1)$th layer is the last to be influenced by the surface and this layer must be contained in the last surface-influenced cell, $(p-1)$. With a cell size of b^{d+1} the $(p-1)$th cell contains the layers $(p-2)b+1$ to $(p-1)b$. The smallest integer p satisfying the inequality

$$(p-2)b+1 \leq p+m-1 \leq (p-1)b \qquad \text{(A1)}$$

or

$$\frac{m}{b-1}+1 \leq p \leq \frac{m}{b-1}+2 \tag{A2}$$

is the required value. In turn $(p+m-1)$ layers of spins are influenced by the surface. Knowing the number of spins influenced by the surface we can determine the number of unique parameters needed for the description of the renormalized Hamiltonian.

When we start with a system of b^t layers and reduce the number of layers by a factor b with each renormalization we arrive, after $\hat{t}$ transformations, at a system with no bulk spins so that $b^{t-\hat{t}} \leq 2(p+m-1)$. Different renormalization equations will be needed for the $(\hat{t}+1)$th to tth transformations. If the $(\hat{t}-1)$th renormalization results in less than $b(2p+m-2)$ layers, the mth-order term in the cumulant expansion must contain interactions between a cell influenced by one surface and a cell influenced by the other surface. In this case the $\hat{t}$ th renormalization also requires a separate set of equations. This occurs for $m=1$, $b=\geq 4$, with $\hat{t}=t$; $m=2$, $b=3$, with $\hat{t}=t-1$; $m=3$, $b=2$ with $\hat{t}=t-3$; and $m=4$, $b=5$, with $\hat{t}=t-1$. In the cases when there are $b(2p+m-2)$ or more spin layers, the same renormalizations as used in the 1st to $(\hat{t}-1)$th renormalizations can be used in the $\hat{t}$ th renormalization. This occurs for $m=1$, $b=3,4$; $m=2,3$, $b=4,5,6$; $m=4$, $b=4,6$, all with $\hat{t}=t-1$; $m=1$, $b=2$; $m=3,4$, $b=3$, with $\hat{t}=t-2$; $m=2$, $b=2$, with $\hat{t}=t-3$; and $m=4$, $b=2$, with $\hat{t}=t-4$.

Next we discuss the calculation of the derivatives of the free energy of the original system with respect to the starting parameters, in terms of the free energy of the collapsed system with respect to renormalized parameters. For convenience we adopt a vector notation and let $\vec{\mu}(k)=[J_B(k),h_B(k),\ldots,]$ be the vector containing the bulk spin coupling parameters after k renormalizations. In general $\vec{\mu}(k)$ will contain additional parameters such as diagonal and next-to-nearest-neighbor couplings, etc. Let

$$\vec{\tau}(k)=[J_1(k),\ldots,J_i(k),\ldots,h_1(k),\ldots,h_i(k),\ldots,]$$

be the vector containing the remaining parameters that describe interactions involving nonbulk spins. Finally, $\vec{g}(k)=[g_1(k),\ldots,g_{p-1}(k)]$ contains the nonbulk cell constants generated by the kth renormalization, and $g_B(k)$ is the corresponding bulk cell constant.

Since the parameters for the surface do not appear in the renormalization equations for the bulk parameters, we have the following relations for $k \leq \hat{t}-1$ and all (i,j):

$$\frac{\partial g_B(k)}{\partial g_i(k-1)}=\frac{\partial g_B(k)}{\partial \tau_i(k-1)}=\frac{\partial \mu_j(k)}{\partial g_i(k-1)}$$

$$=\frac{\partial \mu_j(k)}{\partial \tau_i(k-1)}=0 \tag{A3}$$

and since the cell constants do not appear in the equations for the coupling parameters we also find

$$\frac{\partial \mu_j(k)}{\partial g_B(k-1)}=\frac{\partial \tau_j(k)}{\partial g_B(k-1)}=\frac{\partial \tau_j(k)}{\partial g_i(k-1)}=0 \ . \tag{A4}$$

We can obtain recursion relations for the first partial derivatives linking the parameters after k transformation from the following chain rules, making use of Eqs. (A3) and (A4), as well as the summation convention over repeated indices,

$$\frac{\partial \mu_j(k)}{\partial \mu_i(0)}=\frac{\partial \mu_j(k)}{\partial \mu_l(k-1)}\frac{\partial \mu_l(k-1)}{\partial \mu_i(0)} \ , \tag{A5a}$$

$$\frac{\partial \tau_j(k)}{\partial \mu_i(0)}=\frac{\partial \tau_j(k)}{\partial \mu_l(k-1)}\frac{\partial \mu_l(k-1)}{\partial \mu_i(0)}+\frac{\partial \tau_j(k)}{\partial \tau_l(k-1)}\frac{\partial \tau_l(k-1)}{\partial \mu_i(0)} \ , \tag{A5b}$$

$$\frac{\partial \tau_j(k)}{\partial \tau_i(0)}=\frac{\partial \tau_j(k)}{\partial \tau_l(k-1)}\frac{\partial \tau_l(k-1)}{\partial \tau_i(0)} \ , \tag{A5c}$$

$$\frac{\partial g_B(k)}{\partial \mu_i(0)}=\frac{\partial g_B(k)}{\partial g_B(k-1)}\frac{\partial g_B(k-1)}{\partial \mu_i(0)}+\frac{\partial g_B(k)}{\partial \mu_l(k-1)}\frac{\partial \mu_l(k-1)}{\partial \mu_i(0)} \ , \tag{A5d}$$

$$\frac{\partial g_j(k)}{\partial \mu_i(0)}=\frac{\partial g_j(k)}{\partial g_B(k-1)}\frac{\partial g_B(k-1)}{\partial \mu_i(0)}+\frac{\partial g_j(k)}{\partial \mu_l(k-1)}\frac{\partial \mu_l(k-1)}{\partial \mu_i(0)}+\frac{\partial g_j(k)}{\partial g_l(k-1)}\frac{\partial g_l(k-1)}{\partial \mu_i(0)}+\frac{\partial g_j(k)}{\partial \tau_l(k-1)}\frac{\partial \tau_l(k-1)}{\partial \mu_i(0)} \ , \tag{A5e}$$

$$\frac{\partial g_j(k)}{\partial \tau_i(0)}=\frac{\partial g_j(k)}{\partial g_l(k-1)}\frac{\partial g_l(k-1)}{\partial \tau_i(0)}+\frac{\partial g_j(k)}{\partial \tau_l(k-1)}\frac{\partial \tau_l(k-1)}{\partial \tau_i(0)} \ . \tag{A5f}$$

For the second derivatives we have the following solutions, similar to Eqs. (A3) and (A4), where X is

an element of $\vec{\mu}(k)$, $\vec{\tau}(k)$, $\vec{g}(k)$, or $g_B(k)$, and Y is an element of $\vec{\mu}(k-1)$, $\vec{\tau}(k-1)$, $\vec{g}(k-1)$, or $g_B(k-1)$:

$$\frac{\partial^2 X}{\partial g_B(k-1)\partial Y}=\frac{\partial^2 X}{\partial g_i(k-1)\partial Y}=\frac{\partial^2 g_B(k)}{\partial \tau_i(k-1)\partial Y}=\frac{\partial^2 \mu_B(k)}{\partial \tau_i(k-1)\partial Y}=0\ , \tag{A6}$$

for all i, X, Y. Making use of Eq. (A6) we find the following chain rules for the second derivatives:

$$\frac{\partial^2 \mu_j(k)}{\partial \mu_i(0)\partial \mu_l(0)}=\frac{\partial^2 \mu_r(k-1)}{\partial \mu_i(0)\partial \mu_l(0)}\frac{\partial \mu_j(k)}{\partial \mu_r(k-1)}+\frac{\partial \mu_r(k-1)}{\partial \mu_i(0)}\frac{\partial \mu_s(k-1)}{\partial \mu_l(0)}\frac{\partial^2 \mu_j(k)}{\partial \mu_r(k-1)\partial \mu_s(k-1)}\ , \tag{A7a}$$

$$\begin{aligned}\frac{\partial^2 \tau_j(k)}{\partial \mu_i(0)\partial \mu_l(0)}=&\frac{\partial^2 \mu_r(k-1)}{\partial \mu_i(0)\partial \mu_l(0)}\frac{\partial \tau_j(k)}{\partial \mu_r(k-1)}+\frac{\partial^2 \tau_r(k-1)}{\partial \mu_i(0)\partial \mu_l(0)}\frac{\partial \tau_j(k)}{\partial \tau_r(k-1)}\\&+\frac{\partial \mu_r(k-1)}{\partial \mu_i(0)}\frac{\partial \mu_s(k-1)}{\partial \mu_l(0)}\frac{\partial^2 \tau_j(k)}{\partial \mu_r(k-1)\partial \mu_s(k-1)}+\frac{\partial \mu_r(k-1)}{\partial \mu_i(0)}\frac{\partial \tau_s(k-1)}{\partial \mu_l(0)}\frac{\partial^2 \tau_j(k)}{\partial \mu_r(k-1)\partial \tau_s(k-1)}\\&+\frac{\partial \mu_r(k-1)}{\partial \mu_l(0)}\frac{\partial \tau_s(k-1)}{\partial \mu_i(0)}\frac{\partial^2 \tau_j(k)}{\partial \mu_r(k-1)\partial \tau_s(k-1)}+\frac{\partial \tau_r(k-1)}{\partial \mu_i(0)}\frac{\partial \tau_s(k-1)}{\partial \mu_l(0)}\frac{\partial^2 \tau_j(k)}{\partial \tau_r(k-1)\partial \tau_s(k-1)}\end{aligned} \tag{A7b}$$

$$\begin{aligned}\frac{\partial^2 \tau_j(k)}{\partial \mu_i(0)\partial \tau_l(0)}=&\frac{\partial^2 \tau_r(k-1)}{\partial \mu_i(0)\partial \tau_l(0)}\frac{\partial \tau_j(k)}{\partial \tau_r(k-1)}+\frac{\partial \mu_r(k-1)}{\partial \mu_i(0)}\frac{\partial \tau_s(k-1)}{\partial \tau_l(0)}\frac{\partial^2 \tau_j(k)}{\partial \mu_r(k-1)\partial \tau_s(k-1)}\\&+\frac{\partial \tau_r(k-1)}{\partial \mu_i(0)}\frac{\partial \tau_s(k-1)}{\partial \tau_l(0)}\frac{\partial^2 \tau_j(k)}{\partial \tau_r(k-1)\partial \tau_s(k-1)}\ ,\end{aligned} \tag{A7c}$$

$$\frac{\partial^2 \tau_j(k)}{\partial \tau_i(0)\partial \tau_l(0)}=\frac{\partial^2 \tau_r(k-1)}{\partial \tau_i(0)\partial \tau_l(0)}\frac{\partial \tau_j(k)}{\partial \tau_r(k-1)}+\frac{\partial \tau_r(k-1)}{\partial \tau_i(0)}\frac{\partial \tau_s(k-1)}{\partial \tau_l(0)}\frac{\partial^2 \tau_j(k)}{\partial \tau_r(k-1)\partial \tau_s(k-1)}\ , \tag{A7d}$$

$$\begin{aligned}\frac{\partial^2 g_B(k)}{\partial \mu_i(0)\partial \mu_l(0)}=&b^{d+1}\frac{\partial^2 g_B(k-1)}{\partial \mu_i(0)\partial \mu_l(0)}+\frac{\partial^2 \mu_r(k-1)}{\partial \mu_i(0)\partial \mu_l(0)}\frac{\partial g_B(k)}{\partial \mu_r(k-1)}\\&+\frac{\partial \mu_r(k-1)}{\partial \mu_i(0)}\frac{\partial \mu_s(k-1)}{\partial \mu_l(0)}\frac{\partial^2 g_B(k)}{\partial \mu_r(k-1)\partial \mu_s(k-1)}\ ,\end{aligned} \tag{A7e}$$

$$\begin{aligned}\frac{\partial^2 g_j(k)}{\partial \mu_i(0)\partial \mu_l(0)}=&\frac{\partial^2 g_r(k-1)}{\partial \mu_i(0)\partial \mu_l(0)}\frac{\partial g_j(k)}{\partial g_r(k-1)}+\frac{\partial^2 g_B(k-1)}{\partial \mu_i(0)\partial \mu_l(0)}\frac{\partial g_j(k)}{\partial g_B(k-1)}\\&+\frac{\partial^2 \tau_r(k-1)}{\partial \mu_i(0)\partial \mu_l(0)}\frac{\partial g_j(k)}{\partial \tau_r(k-1)}+\frac{\partial^2 \mu_r(k-1)}{\partial \mu_i(0)\partial \mu_l(0)}\frac{\partial g_j(k)}{\partial \mu_r(k-1)}\\&+\frac{\partial \mu_r(k-1)}{\partial \mu_i(0)}\frac{\partial \mu_s(k-1)}{\partial \mu_l(0)}\frac{\partial^2 g_j(k)}{\partial \mu_r(k-1)\partial \mu_s(k-1)}\\&+\frac{\partial^2 g_j(k)}{\partial \mu_r(k-1)\partial \tau_s(k-1)}\left[\frac{\partial \mu_r(k-1)}{\partial \mu_i(0)}\frac{\partial \tau_s(k-1)}{\partial \mu_l(0)}+\frac{\partial \mu_r(k-1)}{\partial \mu_l(0)}\frac{\partial \tau_s(k-1)}{\partial \mu_i(0)}\right]\\&+\frac{\partial^2 g_j(k)}{\partial \tau_r(k-1)\partial \tau_s(k-1)}\frac{\partial \tau_r(k-1)}{\partial \mu_i(0)}\frac{\partial \tau_s(k-1)}{\partial \mu_l(0)}\ ,\end{aligned} \tag{A7f}$$

$$\begin{aligned}\frac{\partial^2 g_j(k)}{\partial \mu_i(0)\partial \tau_l(0)}=&\frac{\partial^2 g_r(k-1)}{\partial \mu_i(0)\partial \tau_l(0)}\frac{\partial g_j(k)}{\partial g_r(k-1)}+\frac{\partial^2 \tau_r(k-1)}{\partial \mu_i(0)\partial \tau_l(0)}\frac{\partial g_j(k)}{\partial \tau_r(k-1)}\\&+\frac{\partial \mu_r(k-1)}{\partial \mu_i(0)}\frac{\partial \tau_s(k-1)}{\partial \tau_l(0)}\frac{\partial^2 g_j(k)}{\partial \mu_r(k-1)\partial \tau_s(k-1)}+\frac{\partial \tau_r(k-1)}{\partial \mu_i(0)}\frac{\partial \tau_s(k-1)}{\partial \mu_l(0)}\frac{\partial^2 g_j(k)}{\partial \tau_r(k-1)\partial \tau_s(k-1)}\ .\end{aligned} \tag{A7g}$$

Now the free energy of the original system of b^t layers can be related to the free energy after $\hat{t}$ transformations by

$$F(0)\equiv F[b^t;\vec{g}(0),\vec{\tau}(0),\vec{\mu}(0)]=b^{-\hat{t}(d+1)}F(\hat{t})\ . \tag{A8}$$

The derivatives with respect to elements of $\vec{\tau}(0)$ or $\vec{\mu}(0)$ are given by

$$\frac{\partial F(0)}{\partial \tau_l(0)} = b^{-\hat{t}(d+1)}\left[\frac{\partial F(\hat{t})}{\partial g_i(\hat{t})}\frac{\partial g_i(\hat{t})}{\partial \tau_l(0)} + \frac{\partial F(\hat{t})}{\partial \tau_i(\hat{t})}\frac{\partial \tau_i(\hat{t})}{\partial \tau_l(0)}\right], \tag{A9}$$

$$\frac{\partial^2 F}{\partial \mu_l(0)\partial \tau_m(0)} = b^{-\hat{t}(d+1)}\left[\frac{\partial^2 F(\hat{t})}{\partial \tau_i(t)\partial \tau_j(\hat{t})}\frac{\partial \tau_i(\hat{t})}{\partial \mu_l(0)}\frac{\partial \tau_j(\hat{t})}{\partial \tau_m(0)} + \frac{\partial F(\hat{t})}{\partial g_i(\hat{t})}\frac{\partial^2 g_i(\hat{t})}{\partial \mu_l(0)\partial \tau_m(0)} + \frac{\partial F(\hat{t})}{\partial \tau_i(\hat{t})}\frac{\partial^2 \tau_i(\hat{t})}{\partial \mu_l(0)\partial \tau_m(0)}\right], \tag{A10}$$

where Eqs. (A5a)–(A5f) and Eqs. (A7a)–(A7g) can be used to compute the partial derivatives, keeping in mind the restriction that when $b^{-t-\hat{t}} < b(2p+m-2)$ the recursion relations for $\vec{g}(\hat{t})$, $\vec{\tau}(\hat{t})$ and the partial derivatives are altered from those used in the first to $(\hat{t}-1)$th transformations.

For each of the $\hat{t}$th to the tth transformations, we calculate the derivatives of the free energy for $b^{t-k'}$ layers, where $\hat{t}+1 < k' < t$, using

$$\frac{\partial F(k'-1)}{\partial \tau_i(k'-1)} = b^{-(d+1)}\left[\frac{\partial F(k')}{\partial g_j(k')}\frac{\partial g_j(k')}{\partial \tau_i(k'-1)} + \frac{\partial F(k')}{\partial \tau_j(k')}\frac{\partial \tau_j(k')}{\partial \tau_i(k'-1)}\right], \tag{A11}$$

$$\frac{\partial F(k'-1)}{\partial g_i(k'-1)} = b^{-(d+1)}\frac{\partial F(k')}{\partial g_j(k')}\frac{\partial g_j(k')}{\partial g_i(k'-1)}, \tag{A12}$$

$$\frac{\partial^2 F(k')}{\partial g_i(k'-1)\partial X} = 0, \quad \text{where } X = g_j(k'-1) \text{ or } \tau_j(k'-1), \tag{A13}$$

$$\frac{\partial^2 F(k'-1)}{\partial \tau_i(k'-1)\partial \tau_j(k'-1)} = b^{-(d+1)}\left[\frac{\partial F(k')}{\partial g_l(k')}\frac{\partial^2 g_l(k')}{\partial \tau_i(k'-1)\partial \tau_j(k'-1)} + \frac{\partial F(k')}{\partial \tau_l(k')}\frac{\partial^2 \tau_l(k')}{\partial \tau_i(k'-1)\partial \tau_j(k'-1)} + \frac{\partial^2 F(k')}{\partial \tau_l(k')\partial \tau_r(k')}\frac{\partial \tau_l(k')}{\partial \tau_i(k'-1)}\frac{\partial \tau_r(k')}{\partial \tau_j(k'-1)}\right]. \tag{A14}$$

The equations (A3)–(A14) are used in the following manner to obtain the desired derivatives of $F(0)$ with the least amount of computation. Suppose the calculation has been carried out for thickness $a(b^{t-1}-1)$ and we have already evaluated $g_B(\hat{t}-2)$, $\vec{\tau}(\hat{t}-2)$, $\vec{\mu}(\hat{t}-2)$, $\vec{g}(\hat{t}-2)$, $\partial g_B(\hat{t}-2)/\partial X$, etc., where $\partial/\partial X$ denotes differentiation with respect to elements of $\vec{\mu}(0)$ or $\vec{\tau}(0)$. We now compute $g_B(\hat{t}-1)$, $\vec{\tau}(\hat{t}-1)$, $\vec{\mu}(\hat{t}-1)$, $g(\hat{t}-1)$, $\vec{g}(\hat{t})$, $\vec{\tau}(\hat{t})$, $\partial g_B(\hat{t}-1)/\partial g_B(\hat{t}-2)$, $\partial g_i(\hat{t})/\partial \tau_j(\hat{t}-1)$, etc., and apply the chain rules (A5a)–(A5f) and (A7a)–(A7g) to obtain $\partial g_B(\hat{t})/\partial X$, etc. We now calculate, in turn, $\vec{g}(k')$, $\vec{\tau}(k')$, $\partial g_B(k')/\partial g_B(k'-1)$, etc., for $\hat{t}+1 \le k' \le t$. Finally we compute $F(t)$ and its derivatives for the system of smaller dimensionality d and with parameters $\vec{g}^*(t)$ and $\vec{\tau}^*(t)$. Equations (A11)–(A14) then give the derivatives of $F(t-1)$, $F(t-2), \ldots, F(\hat{t})$ in turn. Equations (A9) and (A10) can now be used, together with the numerical values of $\partial \tau_i(\hat{t})/\partial X$, etc. Thus, we arrive at the derivatives of $F(0)$ in terms of the original parameters $\vec{\mu}(0)$ and $\vec{\tau}(0)$. The entire procedure can be easily programmed on a computer by using matrix algebra.

[1] L. P. Kadanoff, Physics (N.Y.) 2, 263 (1966).

[2] K. G. Wilson, Phys. Rev. B 4, 3174 (1971); K. G. Wilson and J. Kogut, Phys. Rep. C 12, 75 (1974).

[3] T. Niemeijer and J. M. J. Van Leeuwen, in *Phase Transitions and Critical Phenomena*, edited by C. Domb and M. S. Green (Academic, London, 1976), Vol. 6.

[4] This approach has been independently applied by R. Cordery (unpublished notes) to the simplest case of a bounded system using a first-order cumulant expansion in the absence of both surface terms and a magnetic field.

[5] G. F. Newell and E. W. Montroll, Rev. Mod. Phys. 25, 353 (1953).

[6] M. E. Fisher and M. N. Barber, Phys. Rev. Lett. 28, 1516 (1972).

[7] K. Binder and P. C. Hohenberg, Phys. Rev. B 9, 2194 (1974).

[8] Equation (4) of L. G. Dunfield and J. Noolandi, Solid State Commun. 32, 441 (1979) contains a misprint which has been corrected in Eq. (18) of the present work.

[9] A. L. Lewis, Phys. Rev. B 18, 5091 (1978).

[10]R. P. Feynman, *Statistical Mechanics, A Set of Lectures* (Benjamin, Reading, Mass., 1972), pp. 136–150.
[11]S. Hsu and J. D. Gunton, Phys. Rev. B 15, 2688 (1977).
[12]B. Nienhuis and M. Nauenberg, Phys. Rev. B 11, 4152 (1975).
[13]C. Domb, in *Phase Transitions and Critical Phenomena,* edited by C. Domb and M. S. Green (Academic, New York, 1974), Vol. 3.
[14]S. Katsura, N. Yazaki, and M. Takaishi, Can. J. Phys. 55, 1648 (1977).
[15]S. McKenzie, Can. J. Phys. 57, 1239 (1979).
[16]S. Ma, *Modern Theory of Critical Phenomena* (Benjamin, Reading, Mass., 1976).
[17]M. E. Fisher, J. Vac. Sci. Technol. 10, 665 (1973).
[18]Figures 2 and 3 of L. G. Dunfield and J. Noolandi, Solid State Commun. 32, 441 (1979) show the wrong signs for λ. However, the correct values of λ are given in the text of this reference.
[19]M. E. Fisher, in *Proceedings of the 51st Enrico Fermi Summer School, Varenna, 1970,* edited by M. S. Green (Academic, New York, 1971).
[20]A. J. Bray and M. A. Moore, J. Phys. A 11, 715 (1978).
[21]H. Au-Yang and M. E. Fisher, Phys. Rev. B 11, 3469 (1975).
[22]T. W. Capehart and M. E. Fisher, Phys. Rev. B 13, 5021 (1976).
[23]L. G. Dunfield and J. Noolandi (unpublished).